Improved Fracture Resistance of Cu/Mo Bilayers with Thickness Tailoring

Megan J. Cordill[a,b*], Tanja Jörg[b], Daniel M. Többens[c], Christian Mitterer[b]

[a] Erich Schmid Institute of Materials Science, Austrian Academy of Sciences, Jahnstrasse 12, 8700 Leoben, Austria

[b] Department of Materials Science, Montanuniversität Leoben, Franz-Josef-Strasse 18, 8700 Leoben, Austria

[c] Helmholtz-Zentrum Berlin für Materialien und Energie (HZB), Albert-Einstein-Str. 15, 12489 Berlin, Germany

* Corresponding author: megan.cordill@oeaw.ac.at

Abstract

The fracture toughness of Mo in Cu/Mo bilayers on polyimide was assessed with *in situ* X-ray diffraction during uniaxial tensile straining. The fracture resistance of Mo acting as an adhesion layer greatly depends on the thickness of the Cu layer exhibiting a toughening effect with increasing Cu layer thickness. In contrast, the presence of the Mo interlayer greatly decreases the apparent K_{Ic} of the Cu layers. The quantification of K_{Ic} for Mo with a Cu top layer provides further evidence that when brittle layers are used, a thicker ductile layer is advantageous to create fracture resistant stretchable systems.

I. Introduction

For a reliable implementation and future design of flexible, stretchable, and bendable electronics, multilayer thin film architectures need to be examined with emphasis on their damage tolerance. For example, it has been demonstrated that when brittle adhesion layers[1–3] or protective corrosion layers[4] are combined with ductile metals (Cu, Au, Ag, or Al), the fracture behavior of the ductile film is reduced when strained. The reduction is due to the fact that the brittle layers, typically 10-50 nm thick, have a lower fracture strain than the ductile layer and the cracks which form in the brittle layers act as stress concentrators in the ductile film[1–4]. The ductile layer thickness and microstructure have been shown to be deciding factors for the type and amount of deformation which occurs under monotonic[1,3] and cyclic loading[5–7]. The experimental evidence also illustrates a difference in the crack onset strains with and without a brittle layer[1,2]. Within this work, the fracture resistance of single layers of Mo and Cu/Mo bilayers (with Cu on top and Mo on the bottom) on flexible polyimide (PI) substrates will be investigated by observing the behavior of Cu and Mo independently. Our results illustrate that the presence of high strength interlayers, such as thin Mo layers, may reduce the fracture resistance of ductile films.

When the fracture stress of a thin film is known, several models are available to calculate the Mode I fracture toughness, K_{Ic}, of a brittle film[8–13] as the most critical component of the composite structure. Of the available models, that of Beuth[8] is the most promising because it accounts for the elastic mismatch between film and substrate, which is taken into account by the Dundur's parameters, α and β[14]. Using the steady state energy release rate, G_{ss}, the fracture resistance of an individual layer can be evaluated with Eqn. 1,

$$G_{ss} = \frac{\pi\sigma^2 h}{2E_f'} g(\alpha,\beta), \tag{1}$$

where σ_f is the fracture stress of the film, h is the film thickness, $E_f' = E_f/(1-\nu_f^2)$ with E_f is the elastic modulus of the film, ν_f is the Poisson's ratio of the film, and $g(\alpha,\beta)$ is a dimensionless parameter based on the Dundur's parameters α and β[8,14]. Finally, the equivalent fracture toughness in terms of K_{Ic} is determined with the relationship: $K_{Ic}^2 = G_{ss}E_f'$.

In order to determine quantitatively how the Mo layer influences the fracture resistance of the bilayer, *in situ* tensile straining with X-ray diffraction (XRD) was utilized[1,15–17]. With this technique the lattice strains developing in both the Mo and Cu layers can be measured independently with the $\sin^2\psi$ method[18]. From the measured lattice strains individual film stresses as a function of the applied engineering strain were calculated. The evolution of the measured stresses in single ductile or brittle layers as well as bilayers (ductile with brittle interlayers) is well understood[1,2,4,13,15,17,19]. It will be demonstrated using Cu/Mo bilayers with different thickness ratios that the apparent fracture toughness of the Mo layer increased as the thickness of the ductile Cu layer increased according to the model of Beuth[8].

II. Experimental Procedures

Bilayers of Cu and Mo were sputter deposited onto 50 µm thick PI (UBE UPILEX-S 50S) and 350 µm thick Si (100) substrates. The Mo layer was held constant at 50 nm and was used as an adhesion layer for the ductile Cu layers, which were 50, 150, 300, and 500 nm thick. For comparison, single layer films (50 nm Mo and 50, 150, 300, and 500 nm Cu, corresponding to Cu/Mo thickness ratios of 1:1, 3:1, 6:1, and 10:1) were also deposited using the same deposition parameters as the bilayers. Single and bilayers were grown using a lab-scale direct current (d.c.) magnetron sputter deposition system equipped with three unbalanced 2-inch diameter magnetrons using two Mo and one Cu target, which are focused towards the center of a rotatable sample holder. Substrates were ultrasonically cleaned in ethanol for 5 min and afterwards dried in hot air, before mounting them with Kapton tape to the center of the rotatable substrate holder, which was kept at floating potential without applying external heating. The vacuum chamber was evacuated to a base pressure of less than 1×10^{-3} Pa. Before film deposition, substrates were Ar ion etched at a pressure of 1 Pa using an asymmetrically bipolar pulsed d.c. discharge at a substrate voltage of -350 V and a frequency of 50 kHz for 2 min. The films were synthesized by applying a d.c. current of 0.35 A on each Mo target (Mo films) and of 0.35 A on the Cu target (Cu films) at a constant Ar pressure of 0.36 Pa. The above-mentioned deposition parameters led to deposition times of 56 s for the 50 nm Mo thin film and for the Cu thin films for a layer thickness of 50 nm (58 s), 150 nm (2 min 53 s), 300 nm (4 min 14 s) and 500 nm (7 min 22 s). Film thickness measurements were performed using a stylus surface profiler (Veeco DEKTAK 150).

In situ tensile straining with XRD and four point probe (4PP) resistance measurements using an Anton Paar TS600 were performed at the synchrotron beamline KMC-2, BESSY II, Berlin[20]. All samples were strained to 12% while continuously measuring the electrical resistance and collecting XRD patterns for the Mo 110 peak and/or Cu 111 peak (simultaneously for the bilayers) using a Bruker VÅNTEC 2000 area detector and a beam wavelength of 0.154 nm. With the $\sin^2\psi$ method[18], five different ψ angles between 0 and 50 degrees were measured consecutively with an exposure time of 5 s. The peak positions and widths were determined using a Pearson fit and the Mo and Cu film stresses were calculated using X-ray elastic constants (XECs) (1/2 S_2)[21] for untextured 111 Cu and 110 Mo reflections. XECs were calculated from single-crystal elastic constants assuming the Hill model with the software ElastiX[22]. After straining, scanning electron microscopy (SEM) and focused ion beam (FIB) cross-sections were used to characterize the surface and sub-surface deformation and cracking, as well as confirm the film thicknesses.

III. Results and Discussion

Straining of the single layers up to 12% revealed fragmentation of the Mo film whereas the Cu films stayed intact. For the 50 nm Mo film, the stresses increase to a certain level and then drop off to a plateau value (Figure 1a). Film fracture occurs at the maximum stress (confirmed by the resistance data, Figure 1a) causing the stress to decrease due to the through thickness crack formation until crack saturation is reached (stress plateau). The XRD stress-strain curves for the Cu films (Figure 1a) also reach a maximum stress, that increases as the film thickness decreases (a smaller is stronger trend[23]), however, without showing fragmentation. After achieving the maximum value, the stresses saturate, which is characteristic of ductile thin film deformation[13,15,16,19]. The different facture behavior of the brittle Mo thin films and the ductile Cu films is also evidenced by the electrical resistance data shown in Figure 1a [24,25]. While the 50 nm brittle Mo cracked around 1.6% engineering strain, as shown by the

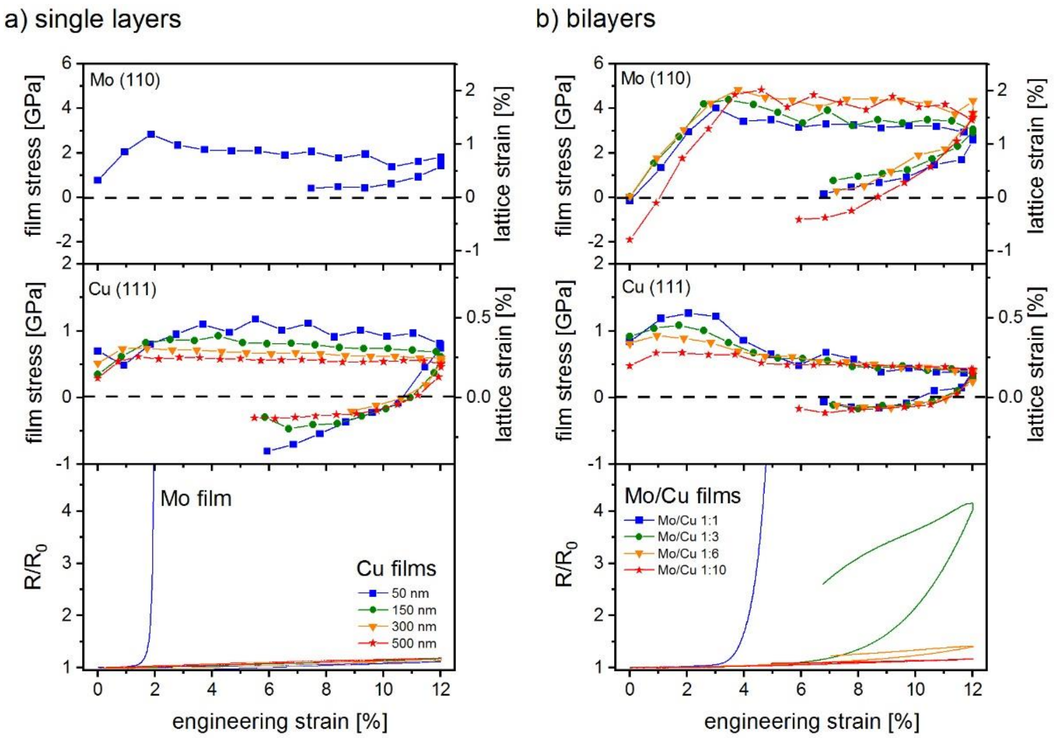

Figure 1: (a) Single layer Mo and Cu stress and resistance ratio evolutions as a function of engineering strain. The Mo film fractures at about 1.6% engineering strain and is evidenced by the stress decrease and strong resistance ratio increase. The single Cu films illustrate common ductile behavior and no significant resistance ratio increase, indicating no through thickness crack formation. (b) Cu/Mo bilayer stress and resistance ratio evolutions as function of engineering strain. Mo interlayer achieve slightly higher maximum stresses, but still fracture, as viewed by the Mo stress decrease. The thin Cu layers also have stress decreases and resistance ratio increases both characteristic of through thickness crack formation.

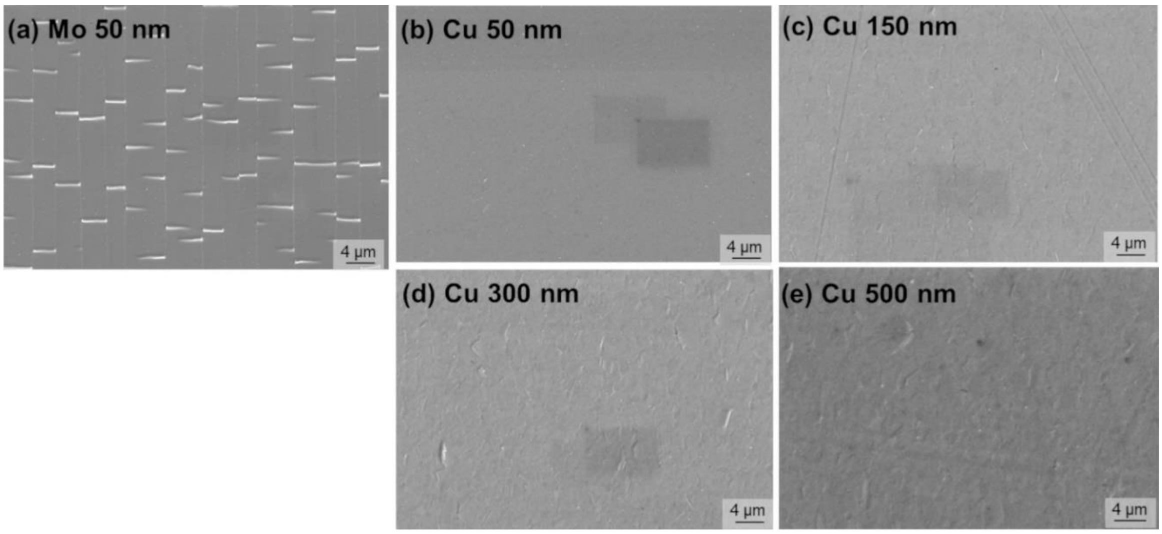

Figure 2: SEM images of single layer films after straining up to 12 %. (a) 50 nm Mo film has through thickness cracks and buckles, while the Cu films, (b) 50 nm, (c) 150 nm, (d) 300 nm, and (e) 500 nm, only have uniform surface deformation and no through thickness cracks.

large increase in the resistance ratio (R/R_0), no increase in resistance ratio is observed in the Cu films. Post-straining SEM images (Figure 2) confirm cracks in the Mo film and uniform deformation in the Cu films with no through thickness cracks.

The stress-strain behavior of the Cu films in the bilayer samples transitions from brittle (1:1 film thickness ratio) to a ductile response (10:1 film thickness ratio) as the Cu thickness increases (Figure 1b), as demonstrated by the electrical resistance. Again, the Mo film in the bilayer has a mostly brittle behavior reaching a maximum stress, then dropping to a lower stress and a plateau. Electrical resistance data illustrates that the fracture behavior of the bilayers depends on the Cu thickness, where the thinner Cu layer resistance ratio changes slope, indicating through thickness cracking[3]. Note that the electrical resistance measured is the response of the Cu layer rather than the Mo layer in the bilayers. Figure 3 contains SEM micrographs of the strained bilayer films, demonstrating that the Cu surfaces of the bilayers only have localized deformation, also called necks, and no through thickness cracks except for the 1:1 Cu/Mo film system. The increased Cu thickness aids in suppressing the through thickness crack growth induced by the cracked Mo layer. Similar behavior was observed for Al/Mo bilayers on polyimide[3] and is demonstrated by FIB cross-sections (Figure 4).

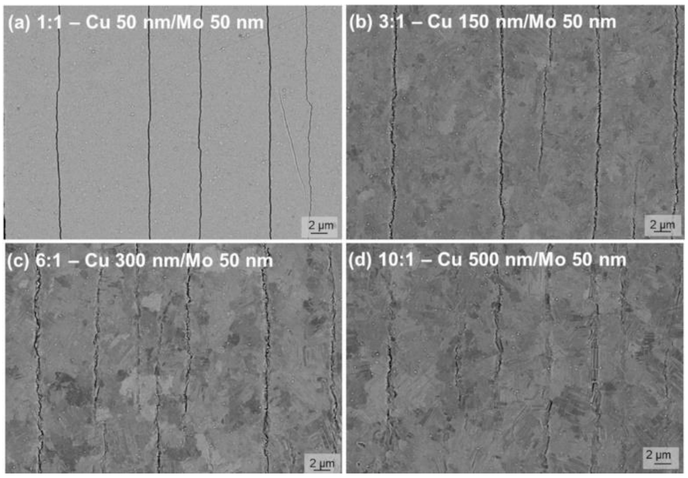

Figure 3: SEM images of bilayer films after straining up to 12 % for bilayer thickness ratios of (a) 1:1, (b) 3:1, (c) 6:1, and (d) 10:1. According to the *in situ* 4PP results (Figure 1) all bilayers except for the 10:1 have through thickness cracks.

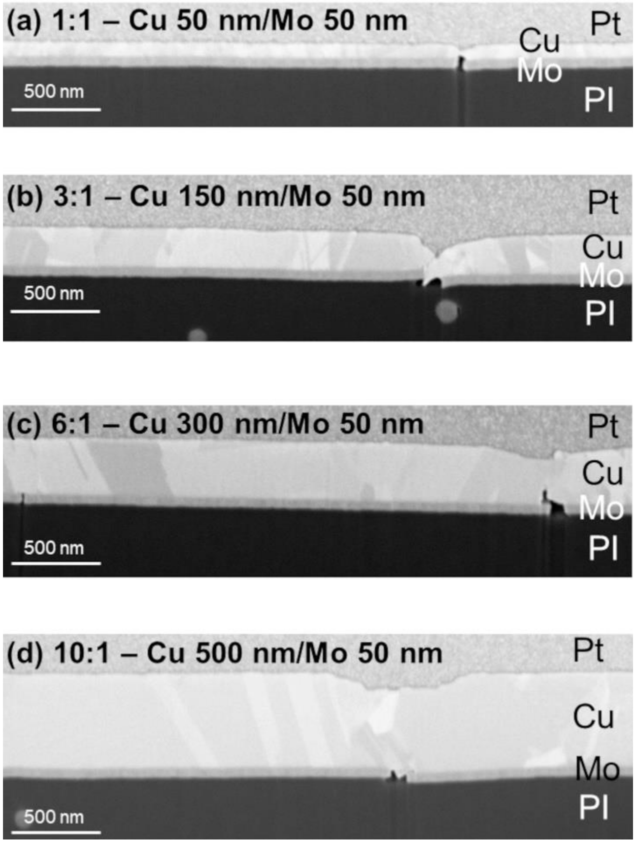

Figure 4: (a) FIB cross-sections of the bilayers after straining illustrating cracks in the Mo layer and localized deformation (necking) in the Cu layers, which can impede the growth of the Mo cracks.

Using the maximum stress from the *in situ* XRD experiments and the elastic constants for Mo, Cu and PI, the G_{ss} and K_{Ic} of the Mo in the Cu/Mo bilayers was evaluated. First, the Dundur's parameter α was determined for the Mo-PI interface (α = 0.9832) in order to employ the correct dimensionless parameter $g(\alpha, \beta)$ from Table 2 found by Beuth[8], which also shows that β has a negligible influence on $g(\alpha, \beta)$ and is assumed to be zero. With $g(\alpha, \beta) = 22.68$, the single layer Mo film has a fracture toughness K_{Ic} of 4 MPa·m$^{1/2}$. Compared to the single layer, the apparent K_{Ic} of the Mo layer in the Cu/Mo bilayers increased with increasing Cu thickness (5.3 to 6.7 MPa·m$^{1/2}$) as shown in Figure 5. A possible plateau of K_{Ic} appears to be achieved with a Cu thickness of 300 nm, or a Cu to Mo film thickness ratio of 1:6. The continued Mo crack propagation is a balance between the opening of the Mo cracks and the deformation of the Cu layer above the Mo cracks. It has been quantitatively measured that the fracture behavior of an interlayer or adhesion layer (i.e. Mo) in a metal-polymer system is improved when combined with a ductile layer.

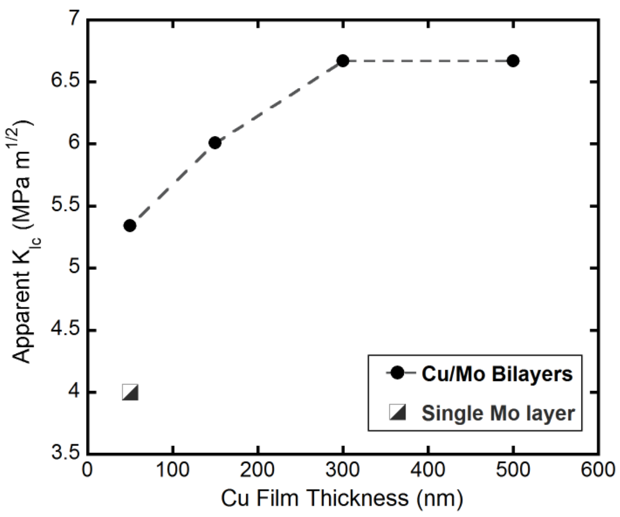

Figure 5: Calculated apparent fracture toughness of the 50 nm Mo layer without and with a Cu layer.

IV. Conclusions

The implications of how the fracture resistance for Mo and Cu single and bilayer films are influenced is twofold. On one hand, it is beneficial that the overlying ductile layer increases the apparent fracture toughness K_{Ic} of the Mo film, which is reflected in the measured initial fracture strain. The results indicate that thicker ductile layers should be utilized for improved electro-mechanical behaviour of bilayers or in multilayer architectures. However, the increased film thickness is only effective to a certain point. For example, for the Cu/Mo bilayer system the optimum film thickness ratio is 6:1 according to K_{Ic}. On the other hand, when thinner ductile layers are used, the combined electro-mechanical reliability of the ductile layer is greatly reduced compared to single layer films of the same thickness. Overall, it has been quantitatively demonstrated that for stretchable applications, especially where the applied loading is uniaxial tension, the best architecture for an electrically conductive ductile metal is a single layer with good adhesion to the polymer substrate. If brittle metal layers are necessary as adhesion promoters, thicker ductile layers are recommended.

Acknowledgements

The authors would like to acknowledge Helmholtz Zentrum Berlin for the allocation of synchrotron radiation beam time and financial support (projects 15202990-ST/R-1.1-P and 16224035-ST). Funding for this research has been provided by the Österreichische Forschungsförderungsgesellschaft mbH within the framework of the Headquarters project E^2SPUTTERTECH (project number 841482). J. Winkler and H. Köstenbauer are gratefully acknowledged as well.

Data Availability Statement

The data that support the findings of this study are available from the corresponding author upon reasonable request.

References

[1] V.M. Marx, F. Toth, A. Wiesinger, J. Berger, C. Kirchlechner, M.J. Cordill, F.D. Fischer, F.G. Rammerstorfer, and G. Dehm, Acta Mater. **89**, 278 (2015).

[2] B. Putz, R.L. Schoeppner, O. Glushko, D.F. Bahr, and M.J. Cordill, Scr. Mater. **102**, 23 (2015).

[3] P. Kreiml, M. Rausch, V.L. Terziyska, H. Köstenbauer, J. Winkler, C. Mitterer, and M.J. Cordill, Thin Solid Films **665**, 131 (2018).

[4] B. Putz, C. May-Miller, V. Matl, B. Völker, D.M. Többens, C. Semprimoschnig, and M.J. Cordill, Scr. Mater. **145**, 5 (2018).

[5] M.J. Cordill, O. Glushko, A. Kleinbichler, B. Putz, D.M. Többens, and C. Kirchlechner, Thin Solid Films **644**, 166 (2017).

[6] O. Glushko and M.J. Cordill, JOM **66**, 598 (2014).

[7] O. Glushko, A. Klug, E.J.W. List-Kratochvil, and M.J. Cordill, Mater. Sci. Eng. A **662**, 157 (2016).

[8] J.L. Beuth, Int. J. Solids Struct. **29**, 1657 (1992).

[9] J.L. Beuth and N.W. Klingbeil, J. Mech. Phys. Solids **44**, 1411 (1996).

[10] J.W. Hutchinson and Z. Suo, Adv. Appl. Mech. **29**, 63 (1992).

[11] T. Ye, Z. Suo, and A.G. Evans, Int. J. Solids Struct. **27**, 2639 (1992).

[12] S. Olliges, P.A. Gruber, S. Orso, V. Auzelyte, Y. Ekinci, H.H. Solak, and R. Spolenak, Scr. Mater. **58**, 175 (2008).

[13] P.A. Gruber, E. Arzt, and R. Spolenak, J. Mater. Res. **24**, 1906 (2009).

[14] J. Dundurs, J. Appl. Mech. **36**, 650 (1969).

[15] B. Putz, O. Glushko, V.M. Marx, C. Kirchlechner, D. Toebbens, and M.J. Cordill, MRS Adv. **1**, 773 (2016).

[16] T. Jörg, M.J. Cordill, R. Franz, C. Kirchlechner, D.M. Többens, J. Winkler, and C. Mitterer, Mater. Sci. Eng. A **697**, 17 (2017).

[17] M.J. Cordill, A. Kleinbichler, B. Völker, P. Kraker, D.R. Economy, D. Többens, C. Kirchlechner, and M.S. Kennedy, Mater. Sci. Eng. A **735**, 456 (2018).

[18] L. Spieß, G. Teichert, R. Schwarzer, H. Behnken, and C. Genzel, Teubner, Wiesbad. (2005).

[19] J. Berger, O. Glushko, V.M. Marx, C. Kirchlechner, and M.J. Cordill, JOM **68**, (2016).

[20] D. Többens and S. Zander, J. Large-Scale Res. Facil. **2**, 1 (2016).

[21] I.C. Noyan and J.B. Cohen, *Residual Stress: Measurement by Diffraction and Interpretation* (Springer-Verlag, New York, 2013).

[22] H. Wern, N. Koch, and T. Maas, in *Mater. Sci. Forum* (2002), pp. 127–132.

[23] A. Misra, J.P. Hirth, and R.G. Hoagland, Acta Mater. **53**, 4817 (2005).

[24] N. Lu, X. Wang, Z. Suo, and J.J. Vlassak, Appl. Phys. Lett. **91**, 221909 (2007).

[25] O. Glushko and M.J. Cordill, Exp. Tech. **40**, 303 (2016).